EC-PC spike detection for high performance Brain-Computer Interface

Wing-kin Tam[1,2], Rosa So[3], Cuntai Guan[3], and Zhi Yang[2]

Abstract— **Spike detection is often the first step in neural signal processing. It has profound effects on subsequent steps down the signal processing pipeline. Most existing spike detection algorithms require manual setting of detection threshold, which is very inconvenient for long-term neural interface. Furthermore, these algorithms are usually only evaluated using simulated dataset. Few studies are devoted to evaluating how different spike detection algorithms affect decoding performance in brain-computer interface. We have proposed a new spike detection algorithm called "exponential component - power component" (EC-PC) that offers fully automatic unsupervised spike detection. In this study, we compared the performance of a motor decoding task when different spike detection algorithms were used. EC-PC is shown to produce a higher decoding accuracy compared with other existing algorithms. Our results suggest that EC-PC can help improve motor decoding performance of brain-computer interface.**

I. Introduction

To detect spikes in extracellular neural recording is a challenging problem. The recorded signal is often heavily contaminated by background neural noise. Its signal to noise ratio may also change over time as the glial cells encapsulate the implanted microelectrodes [1]. Currently, many algorithms have been proposed for spike detection, e.g. root-mean-square, Nonlinear Energy Operator (NEO) [2], median threshold[3], continuous waveform transform [4] etc.

However, existing spike detection methods are not without their shortcomings. Firstly, most of the aforementioned methods are supervised in the sense that they require the user to manually set the threshold for detection. Such manual intervention is not desirable for long term neural recordings because the optimal threshold may change over time as the signal-to-noise ratio of the recordings deteriorate. Secondly, some of the existing methods (e.g. median-based threshold, continuous-wavelet transform) are difficult to implement online in integrated circuits, either due to demanding memory requirements or high computational complexity. Therefore, there is a need for an accurate, efficient spike detection algorithm that can be implemented online. Thirdly, many spike detection algorithms are only evaluated on simulated spike signals but not on real data, and hence the validity of the evaluation depends on the assumptions behind the simulation procedures. A better way is to evaluate the performance of various spike detection algorithms on real data acquired during a behaviour task, e.g. motor decoding. A better spike detection algorithm should detect spike more accurately and lead to better performance.

Previously we have proposed a novel spike-detection algorithm called "exponential component-power component" (EC-PC) that is both efficient and accurate [5]. We have shown that it outperformed other methods in simulated data and also demonstrated the feasibility to implement it on an Application-specific Integrated Circuit (ASIC) chip [6]. Here in this study we evaluated the performance of EC-PC in a motor-decoding task using brain computer interface and compared it with other existing spike detection algorithms.

II. Methodology

A. EC-PC decomposition

In a previous study, we have reported that neural noise in intracortical recording tends to follow an exponential distribution while spikes tend to follow a polynomial distribution in the Hilbert space [5]. Mathematically, given a recorded neural data sequence $V(t)$, we can construct an analytic signal using Hilbert transform:

$$V_{st}(t) = V(t) + jH\{V(t)\} = V(t) + j\frac{1}{\pi}\beta\int_{-\infty}^{\infty}\frac{V(\tau)}{t-\tau}d\tau \quad (1)$$

where β is the Cauchy principal value and H denotes the Hilbert transform.

The instantaneous power of the Hilbert transform then is:

$$Z(t) = |V_{st}(t)|^2 \quad (2)$$

We have found that the probability density function of neural noise in Hilbert space follows an exponential function:

$$f_n(Z) \propto e^{-\lambda_1 Z} \quad (3)$$

where λ_1 is a positive real number. (3) can be fitted with a linear function in the log-linear space:

$$ln(f_n(Z)) = ln(a) - \lambda_1 Z \quad (4)$$

where a is a constant.

The presence of spikes in a neural signal makes its distribution deviate from exponential form and turned into a power-law distribution:

$$f_d(Z) \propto Z^{-\lambda_2} \quad (5)$$

where λ_2 is a positive real number. (5) can be fitted with a linear function in the log-log space:

$$ln(f_d(Z)) = ln(b) - \lambda_2 ln(Z) \quad (6)$$

where b is a constant.

[1] NUS Graduate School of Integrative Sciences and Engineering, National University of Singapore, 117597, Singapore

[2] Department of Electrical and Computer Engineering, National University of Singapore,117583, Singapore eleyangz@nus.edu.sg

[3] Department of Neural and Biomedical Technology, Institute for Infocomm Research, A*STAR, 138632, Singapore

978-1-4244-9270-1/15/$31.00 ©2015 IEEE

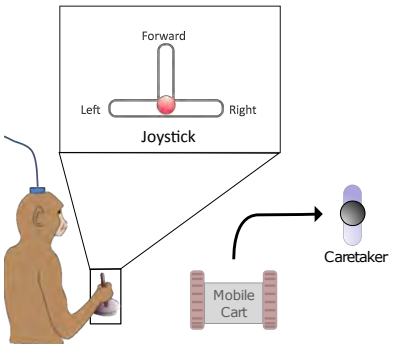

Fig. 1. Experimental setup of the behavioural task. A monkey was trained to use a joystick to control a mobile cart it was sitting on. The movement of the joystick was restricted so that it can only move forward, turn left or right. The objective of the task was to control the mobile cart to reach a caretaker who held a food reward.

Since neural signals consist of both noise and spike, they contain both the exponential component (EC) and power component (PC). Given the EC component $f_n(Z)$ and PC component $f_d(Z)$ fitted from neuron data, the probability of a data point Z_i being a spike can be calculated from:

$$p(Z_i) = \frac{f_d(Z_i)}{f_d(Z_i) + f_n(Z_i)} \tag{7}$$

B. Data acquisition and behavioural task

100-channel microelectrode arrays were implanted into the primary motor cortex of two monkeys. Intracortical neural signals were sampled at 12.5kHz. The two monkeys were trained to sit on a mobile cart and use a joystick to control its movement (Fig. 1). The trajectory of the joystick was restricted such that it can only be pushed forward, left, or right. Pushing the joystick to the left or right turned the mobile cart accordingly. Pushing the joystick forward moved the cart forward. During an experiment session, the caretaker of the monkey was standing at a distance from the monkey while holding a food reward. The monkey was trained to move the mobile cart to reach its caretaker. The monkeys performed the task in multiple sessions per day. Each session consisted of 15-30 trials. The first session of each day's experiment (i.e. the training session) was used as the training set to train a classifier to decode the joystick motion in subsequent sessions (i.e. the testing sessions) for offline analysis. In total, 4 days of experiments were used, 2 for each monkey. Each day of experiment consisted of 1 training session and 1-2 testing sessions. The mobile cart was controlled by the joystick in all sessions. In total there were 7 testing sessions. The experimental procedures involving animal models described in this paper were approved by the Institutional Animal Care and Ethics Committee.

C. Decoding algorithms

Raw signals from the microelectrode array were first bandpass filtered between 300Hz-5000Hz. To capture the changing signal characteristics of the signals, continuous neural recordings were broken down into blocks of 5s. Spike detections were then performed on each of these blocks to extract spikes. Different spike detection methods were used to compare their performance with the EC-PC algorithm. After spike detection, the firing rate of neurons was estimated as follows: in each of the channel, the firing rate was obtained by counting the number of spikes within a 500ms moving window with 100ms overlap and then dividing the spike count by the length of the time window (i.e. 500ms). The firing rates of all channels for a particular time window were then used to construct a feature vector for classification. Afterwards, the class label of that time window was determined by the joystick X and Y coordinates 100ms ahead of the moving window. We labelled each window as Left, Right, Forward or Stop based on the joystick coordinate automatically. The extracted firing rates and class labels were used to train a Support-Vector Machine classifier using LibSVM [7]. We deliberately chose a simple decoding method to ensure that the improvement in performance was mainly due to the ability of the spike detection algorithms in recovering useful information, rather than the capability of the decoding method. The data from the first session of one day's experiments were used to train the SVM classifier. The classification accuracy is defined as the percentage of correctly classified moving windows over total number of moving windows.

D. Comparison with other spike detection algorithms

We compared the decoding accuracy of EC-PC with other popular spike detection algorithms. These algorithms will be briefly described below.

1) Simple threhsold using root-mean-square (RMS): Using a multiple of root-mean-square is the most common method for spike detection. The threshold of detection is set at

$$Threshold = C\sqrt{\frac{1}{N}\sum_{n=1}^{N} x[n]^2} \tag{8}$$

where $x[n]$ is the input neural signal. C is a positive constant. N is the length of the signal

In this study, the above C was set to be 3-5. The value that produced the highest decoding accuracy was used.

2) Simple threshold using median (Median): Qurioga et al. proposes a spike detection method that uses median instead of root-mean-square [3]:

$$\sigma_n = median\left(\frac{|x|}{0.6745}\right) \tag{9}$$

where σ_n is the estimated noise level. The threshold for detection is then set to:

$$Threshold = 4\sigma_n \tag{10}$$

3) Nonlinear energy operator (NEO): Nonlinear energy operator (NEO) gives the instantaneous energy of a signal in the high frequency domain [2]. In discrete time, for input signal $x[n]$ NEO is defined as

$$\psi\{x[n]\} = x[n]^2 - x[n+1]x[n-1] \tag{11}$$

The threshold for spike detection is then set as

$$Threshold = C\frac{1}{N}\sum_{n=1}^{N}\psi[x(n)] \tag{12}$$

In this study, C was chosen to be 10-12. The level that produced the highest decoding accuracy was used.

4) Continuous wavelet transform (CWT): Nenadic and Burdick use continuous wavelet transform for spike detection [4]. A limited set of wavelet scales, based on the length of a typical spike waveform, is used to carry out continuous wavelet transform of a neural signal. Then at each of the transition index and scale, a hypothesis testing is performed according to

$$\text{if} \quad |X(j,k)| < \frac{\hat{\mu}_j}{2} + \frac{\hat{\sigma}_j^{\,2}}{\hat{\mu}_j} log_e \gamma_j \quad \text{accept } H_0, \quad \text{else, accept } H_1 \tag{13}$$

where j is the translation index, k the scale index for scale a_k. H_0 is the hypothesis that the sample only contains noise, and H_1 is the hypothesis that the sample contains both signal (aka spike) and noise. $\hat{\sigma}_j^{\,2}$ is the variance of the noise at scale index j. $\hat{\mu}_j$ is the sample mean of the absolute value of wavelet coefficients under hypothesis H_1. γ_j is a parameter specifying the acceptable level of false alarm and a prior probability of two hypotheses. A data point is considered as spike if at that point H_1 is accepted at multiple scales.

E. Search for the best decoding accuracy

The addition of noisy channels to motor decoding may lower accuracy due to the curse of dimensionality [8]. In this study we determined the highest accuracy a spike detection algorithm can attain using the following method: Motor decoding was performed using each channel individually. The channels were then ranked according to the accuracy obtained using single-channel classification. Using this ranking system, decoding was performed in successive iterations, and the channel with the least information was deleted at each iteration, until the maximum accuracy was achieved.

III. Results

Fig. 2 shows the motor decoding accuracy when different spike detection algorithms were used. As can be seen in Fig.2(a), EC-PC achieved the highest accuracy when all 100 channels of neural signals were used for decoding, attaining an accuracy of 72.4%. EC-PC also produced the lowest standard deviation of decoding performance among algorithms investigated. Fig. 2(b) shows the highest accuracy obtained when low accuracy channels were removed one by one. Again it can be observed that EC-PC obtained the highest accuracy with the lowest standard deviation. It is significantly better than RMS, NEO and CWT, although no significant difference can be observed when compared to the Median method. It should be noted that although continuous wavelet transform produced a very low accuracy when all 100 channels were used for decoding, it achieved comparable accuracy when only the best channels were used.

TABLE I

AVERAGE NUMBER OF CHANNEL HAVING ACCURACY ABOVE CHANCE (I.E. 25%) WHEN ONLY A SINGLE CHANNEL WAS USED FOR DECODING

Methods	No. of channel
EC-PC	72.6
Median	64.3
RMS-4	62.6
NEO-10	60.1
CWT	67.7

TABLE II

THE OPTIMAL THRESHOLD LEVEL OF NONLINEAR ENERGY OPERATOR (NEO) AND MEDIAN THRESHOLD (MEDIAN) THAT ACHIEVED THE HIGHEST DECODING ACCURACY IN EACH OF THE EXPERIMENT SESSION.

Session	NEO	RMS
1	12	5
2	11	5
3	10	5
4	10	4
5	10	4
6	11	4
7	11	3

Table I shows the average number of channels that can produce a decoding accuracy higher than the chance level (i.e. 25%) when only a single channel is used for classification. The values were averaged across all 7 testing sessions. As can be observed, EC-PC produced the highest number of informative channels, with more than 72% of the channels can decode motor movement higher than chance.

We have also tested different thresholding levels for the NEO and Median method. Table II shows the optimal threshold value that produce the highest decoding accuracy in each testing sessions (i.e. the constant C in Equation (12) and (8)). As can be seen, the optimal values varied from session to session. There is no single value that can produce the best performance across all sessions.

IV. Discussion

We have evaluated the performance of various spike detection algorithms in motor decoding using actual intracortical recordings from a behavioural task. We have found that EC-PC produced the highest accuracy compared to other commonly used methods. EC-PC also produced the largest number of informative channels.

The EC-PC algorithm is able to produce the highest decoding accuracy compared to other spike detection methods without any need to manually specify the detection threshold. EC-PC is an automatic and unsupervised method. On the other hand, many existing spike detection algorithms are supervised in the sense that they require manual setting of detection threshold. However, the optimal threshold is highly data dependent and may change over time. For example, our results show that for NEO and RMS, the optimal threshold for decoding is highly data-dependent and change from session to session. EC-PC obviate the need to set the threshold manually. It also achieved the highest accuracy with the lowest standard deviation, meaning that its performance is

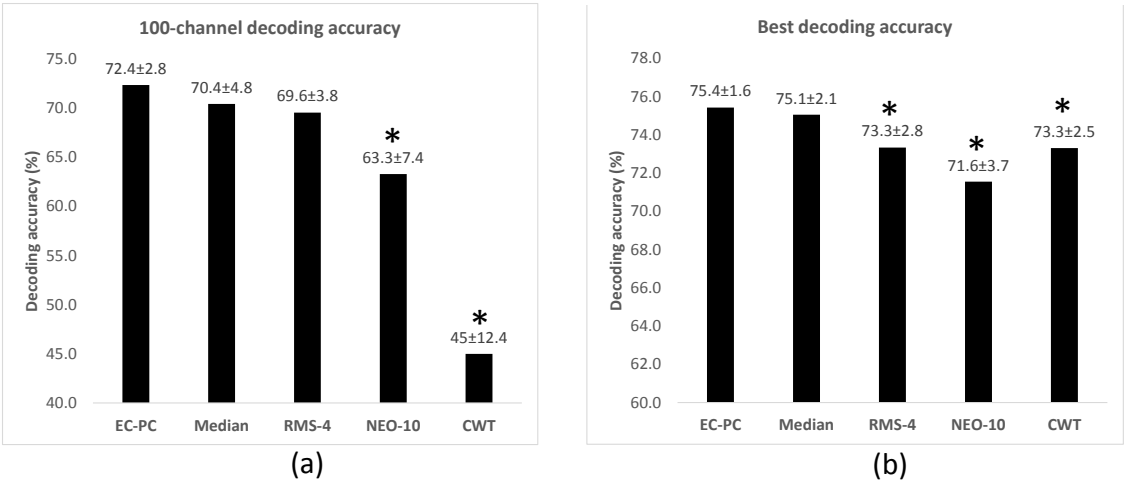

Fig. 2. Comparison of decoding accuracy between different spike detection methods. EC-PC: EC-PC decomposition; Median: median threshold; NEO: Nonlinear Energy Operator; RMS: threshold based on root-mean-square method; CWT: continuous wavelet transform. The number behind NEO and RMS are the threshold level that produce the highest accuracy. NEO was test from 10 to 12 and RMS was tested from 3 to 5 of the threshold level (a) The decoding accuracy when all channels was used (b) The decoding accuracy when low-accuracy channels were removed one by one until the highest accuracy was achieved. Repeated One-way ANOVA shows that there is significant difference among the algorithms used ($p<0.05$). The asterisk (*) indicates that the accuracy of ECPC is significantly higher than that of the indicated method in a post-hoc test ($p<0.05$).

robust across different experimental sessions. It should be noted that the decoding accuracy is lower than a typical invasive BCI because we have included the Stop class, which makes our system akin to an asynchronous BCI.

Our results also suggest that EC-PC can produce more informative channel for classification. More than 70% of the channel extracted by EC-PC are useful for classification in the sense that they can produce an accuracy higher than chance when used individually. This suggest that EC-PC is able to extract more information out of the recording channels. One reason why a more accurate spike detection algorithm can improve motor decoding performance is that it may help to uncover task-relevant neurons that have small spike amplitude. Using conventional spike detection techniques, spikes from such neurons will be considered as noise and be discarded. A more accurate spike detection method like EC-PC can help retain the information content in such neurons and help improve decoding accuracy.

One advantage of implementing on-chip spike detection is that it can drastically cut down on the wireless bandwidth and power consumption of the implanted device, as only spike timings are transmitted. However, some of the existing algorithms, e.g. median threshold and continuous wavelet transform, are difficult to be implemented on chip due to demanding memory and computation power requirements. Recently we have reported an ASIC chip based on EC-PC that been successfully implemented on-chip [6]. The feasibility of implementing EC-PC on-chip coupled with the improved decoding performance reported in this study suggest that EC-PC can be a valuable tool for implantable neural interfaces.

V. CONCLUSIONS

We have used experimental data during a monkey behaviour task to show that EC-PC can produce higher motor decoding accuracy than other existing spike detection algorithms. EC-PC can potentially improve the performance of brain-computer interface applications. One direction for future work is to use EC-PC in online motor decoding to investigate its performance in a full online setting.

REFERENCES

[1] V. S. Polikov, P. A. Tresco, and W. M. Reichert, "Response of brain tissue to chronically implanted neural electrodes," *Journal of Neuroscience Methods*, vol. 148, pp. 1–18, 2005.

[2] S. Mukhopadhyay and G. C. Ray, "A new interpretation of nonlinear energy operator and its efficacy in spike detection." *IEEE transactions on Biomedical Engineering*, vol. 45, no. 2, pp. 180–7, Feb. 1998. [Online]. Available: http://www.ncbi.nlm.nih.gov/pubmed/9473841

[3] R. Q. Quiroga, Z. Nadasdy, and Y. Ben-Shaul, "Unsupervised spike detection and sorting with wavelets and superparamagnetic clustering." *Neural computation*, vol. 16, no. 8, pp. 1661–87, Aug. 2004. [Online]. Available: http://www.ncbi.nlm.nih.gov/pubmed/15228749

[4] Z. Nenadic and J. W. Burdick, "Spike detection using the continuous wavelet transform." *IEEE transactions on Biomedical Engineering*, vol. 52, no. 1, pp. 74–87, Jan. 2005. [Online]. Available: http://www.ncbi.nlm.nih.gov/pubmed/15651566

[5] Z. Yang, W. Liu, M. R. Keshtkaran, Y. Zhou, J. Xu, V. Pikov, C. Guan, and Y. Lian, "A new EC-PC threshold estimation method for in vivo neural spike detection." *Journal of neural engineering*, vol. 9, no. 4, p. 046017, Aug. 2012. [Online]. Available: http://www.ncbi.nlm.nih.gov/pubmed/22791705

[6] Y. Zhou, T. Wu, A. Rastegarnia, C. Guan, E. Keefer, and Z. Yang, "On the robustness of ECPC spike detection method for online neural recording," *Journal of Neuroscience Methods*, vol. 235, pp. 316–330, 2014. [Online]. Available: http://dx.doi.org/10.1016/j.jneumeth.2014.07.006

[7] C. Chang and C. Lin, "LIBSVM: a library for support vector machines," *ACM Transactions on Intelligent Systems and Technology*, vol. 2, no. 3, p. 27, 2011. [Online]. Available: http://www.csie.ntu.edu.tw/ cjlin/libsvm

[8] I. Guyon and A. Elisseeff, "An introduction to variable and feature selection," *J. Mach. Learn. Res.*, vol. 3, pp. 1157–1182, Mar. 2003. [Online]. Available: http://dl.acm.org/citation.cfm?id=944919.944968